

## Original Investigation | ASSOCIATION OF VA SURGEONS

# Effect of Airway Pressure Release Ventilation on Dynamic Alveolar Heterogeneity

Michaela Kollisch-Singule, MD; Sumeet Jain, MD, MBA; Penny Andrews, RN; Bradford J. Smith, PhD; Katharine L. Hamlington-Smith, PhD; Shreyas Roy, MD; David DiStefano, BS; Emily Nuss, BS; Josh Satalin, BS; Qinghe Meng, MD; William Marx, DO; Jason H. T. Bates, PhD; Louis A. Gatto, PhD; Gary F. Nieman, BA; [Nader M. Habashi](#), MD

**IMPORTANCE** Ventilator-induced lung injury may arise from heterogeneous lung microanatomy, whereby some alveoli remain collapsed throughout the breath cycle while their more compliant or surfactant-replete neighbors become overdistended, and this is called dynamic alveolar heterogeneity.

**OBJECTIVE** To determine how dynamic alveolar heterogeneity is influenced by 2 modes of mechanical ventilation: low tidal-volume ventilation (LTVV) and airway pressure release ventilation (APRV), using in vivo microscopy to directly measure alveolar size distributions.

**DESIGN, SETTING, AND PARTICIPANTS** In a randomized, nonblinded laboratory animal study conducted between January 2013 and December 2014, 14 rats (450-500 g in size) were randomized to a control group with uninjured lungs (n = 4) and 2 experimental groups with surfactant deactivation induced by polysorbate lavage: the LTVV group (n = 5) and the APRV group (n = 5). For all groups, a thoracotomy and in vivo microscopy were performed. Following lung injury induced by polysorbate lavage, the LTVV group was ventilated with a tidal volume of 6 mL/kg and progressively higher positive end-expiratory pressure (PEEP) (5, 10, 16, 20, and 24 cm H<sub>2</sub>O). Following lung injury induced by polysorbate lavage, the APRV group was ventilated with a progressively shorter time at low pressure, which increased the ratio of the end-expiratory flow rate (EEFR) to the peak expiratory flow rate (PEFR; from 10% to 25% to 50% to 75%).

**MAIN OUTCOMES AND MEASURES** Alveolar areas were quantified (using PEEP and EEFR to PEFR ratio) to determine dynamic heterogeneity.

**RESULTS** Following lung injury induced by polysorbate lavage, a higher PEEP (20-24 cm H<sub>2</sub>O) with LTVV resulted in alveolar occupancy (reported as percentage of total frame area) at inspiration (39.9%-42.2%) and expiration (35.9%-38.7%) similar to that in the control group (inspiration 53.3%; expiration 50.3%;  $P > .01$ ). Likewise, APRV with an increased EEFR to PEFR ratio (50%-75%) resulted in alveolar occupancy at inspiration (46.7%-47.9%) and expiration (40.2%-46.6%) similar to that in the control group ( $P > .01$ ). At inspiration, the distribution of the alveolar area of the control group was similar to that of the APRV group ( $P > .01$ ) (but not to that of the LTVV group [ $P < .01$ ]). A lower PEEP (5-10 cm H<sub>2</sub>O) and a decreased EEFR to PEFR ratio ( $\leq 50\%$ ) demonstrated dynamic heterogeneity between inspiration and expiration ( $P < .01$  for both) with a greater percentage of large alveoli at expiration. Dynamic alveolar homogeneity between inspiration and expiration occurred with higher PEEP (16-24 cm H<sub>2</sub>O) ( $P > .01$ ) and an increased EEFR to PEFR ratio (75%) ( $P > .01$ ).

**CONCLUSIONS AND RELEVANCE** Increasing PEEP during LTVV increased alveolar recruitment and dynamic homogeneity but had a significantly different alveolar size distribution compared with the control group. By comparison, reducing the time at low pressure (EEFR to PEFR ratio of 75%) in the APRV group provided dynamic homogeneity and a closer approximation of the dynamics observed in the control group.

JAMA Surg. doi:10.1001/jamasurg.2015.2683  
Published online October 7, 2015.

**Author Affiliations:** Department of Surgery, State University of New York Upstate Medical University, Syracuse (Kollisch-Singule, Jain, Roy, DiStefano, Nuss, Satalin, Meng, Marx, Gatto, Nieman); Department of Trauma Critical Care Medicine, R Adams Cowley Shock Trauma Center, University of Maryland School of Medicine, Baltimore (Andrews, Habashi); Department of Medicine, University of Vermont, Burlington (Smith, Hamlington-Smith, Bates); Syracuse Veterans Affairs Medical Center, Syracuse, New York (Marx); Department of Biological Sciences, State University of New York at Cortland, Cortland (Gatto).

**Corresponding Author:** Josh Satalin, BS, Department of Surgery, State University New York Upstate Medical University, 750 E Adams St, Syracuse, NY 13210 (satalinj@upstate.edu).

Despite the development of improved ventilator strategies, the morbidity and mortality associated with acute respiratory distress syndrome (ARDS) remain unacceptably high.<sup>1,2</sup> To prevent ARDS and its associated complications, it is important, first and foremost, to prevent ventilator-induced lung injury by using mechanical ventilation strategies that both maintain alveolar recruitment and avoid tissue overdistension. Protective mechanical ventilation, as it is currently used clinically, aims to avoid overdistension by reducing tidal volume ( $V_t$ ). Nevertheless, regional overdistension of alveolar tissue can still occur when lung mechanical properties become heterogeneous because the  $V_t$  delivered is then forced into tissue regions that have higher compliance. The less compliant regions either remain completely collapsed (atelectatic) or experience damaging cycles of recruitment and derecruitment with each breath.<sup>3</sup> Furthermore, the parenchyma at the boundary between atelectatic and ventilated parenchyma may be subject to increased strain owing to geometric effects.<sup>4</sup> Thus, ventilator-induced lung injury can arise from heterogeneous mechanical behavior at the level of the microanatomy when some alveoli remain collapsed throughout the breath cycle while their more compliant or surfactant-replete neighbors become overdistended.<sup>5</sup> We call this phenomenon *dynamic alveolar heterogeneity*.

Ventilation heterogeneity can be assessed clinically during mechanical ventilation using imaging methods such as computed tomography<sup>6</sup> and electrical impedance tomography.<sup>7</sup> These methods, however, do not have the spatial resolution to reveal dynamic alveolar heterogeneity, so direct visualization of dynamic alveolar heterogeneity in patients is not currently possible. On the other hand, our previous computational modeling work suggests that dynamic alveolar heterogeneity can be predicted from breath-by-breath measurements of lung mechanics following the application of recruitment maneuvers.<sup>8,9</sup> We recently used this approach in a rat model of ARDS<sup>10</sup> to predict how the relative degrees of alveolar overdistension and intratidal derecruitment depend on ventilator settings during both conventional low tidal-volume ventilation (LTVV) and airway pressure release ventilation (APRV). Confirming these predictions experimentally would lend significant support to the validity of assessing dynamic alveolar heterogeneity via computational modeling and would allow for the design of mechanical ventilation strategies that minimize dynamic alveolar heterogeneity.

Accordingly, the purpose of the present study was to quantify dynamic alveolar heterogeneity in a rat model of acute lung injury. We used in vivo microscopy to directly measure intratidal alveolar recruitment during LTVV and APRV and to determine how dynamic alveolar heterogeneity is influenced by these 2 modes of mechanical ventilation and by the settings used with each mode.

## Methods

### Procedure

All experiments were performed in accordance with the National Institutes of Health Guide for the Care and Use of Laboratory

Animals and approved by State University of New York Upstate Medical University Institutional Animal Care and Use Committee. Male Sprague-Dawley rats (450-500 g in size) were acclimated to laboratory conditions for 1 week. Each rat was anesthetized with ketamine hydrochloride (90 mg/mL) and xylazine hydrochloride (10 mg/mL) dosed at 0.1 mg/kg of ketamine. Animals were intubated via tracheostomy with a 2.5-mm tracheal cannula (Harvard Apparatus) and then placed on mechanical ventilation (Dräger Evita Infinity V500) with a positive end-expiratory pressure (PEEP) of 5 cm H<sub>2</sub>O,  $V_t$  = 6 mL/kg, a respiratory rate of 55 breaths/min, and a fraction of inspired oxygen of 21%. The carotid artery was cannulated with silastic tubing for hemodynamic monitoring, and the external jugular vein was cannulated for fluid and medication administration. The right lung was exposed via thoracotomy for in vivo assessment. A microscope coverslip was lowered onto the pleural surface, and the lung was held in place by gentle suction (5 cm H<sub>2</sub>O) for in vivo videomicroscopy (epi-objective microscope with epi-illumination; Olympus America Inc) as previously described.<sup>11</sup> After instrumentation, the rats were randomized into a control group ( $n = 4$ ) or 1 of 2 treatment groups (LTVV [ $n = 5$ ] and APRV [ $n = 5$ ]) using a random number generator (Microsoft Excel), with each group previously assigned an integer value.

### Experimental Groups

#### Control Group

The rats in the control group were maintained on ventilation with PEEP of 5 cm H<sub>2</sub>O, a  $V_t$  of 6 mL/kg, a respiratory rate of 55 breaths/min, and a fraction of inspired oxygen of 21%. The in vivo microscope was placed as already described, and videos were recorded with a high-definition video camera (Allied Visions Stingray, F-145C).

#### Injury

Surfactant deactivation was induced by intratracheal instillation of 0.2% of polysorbate 20 in normal saline (5 mL/kg), half this volume into each lung. The rats were rotated into the right and left lateral decubitus position, respectively, for bilateral polysorbate distribution. The rats were then subjected to injurious mechanical ventilation with high tidal volume ( $V_t$  = 16 mL/kg) and a PEEP of 0 cm H<sub>2</sub>O for 10 minutes. This model of surfactant deactivation would most closely approximate a patient with a direct pulmonary insult, such as pneumonia,<sup>12</sup> aspiration,<sup>13</sup> or inhalation injury.<sup>14</sup> Patients who develop extrapulmonary lung injury are susceptible to surfactant deactivation by way of an indirect injury, and this model may still be applicable; however, it does not encompass the full spectrum of pathophysiologic changes associated with indirect lung injury.<sup>15</sup>

#### LTVV Group

Following injury induced by polysorbate lavage, the rats in this group were switched to LTVV with  $V_t$  = 6 mL/kg, a respiratory rate of 55 breaths/min, and a PEEP of 5 cm H<sub>2</sub>O that is incrementally increased (to 10, 16, 20, and 24 cm H<sub>2</sub>O). The rats were ventilated at each setting for 5 minutes to allow acclimatization. The in vivo microscope was placed as already described, and videos were recorded for 5 ventilator cycles at each ventilation setting.

### APRV Group

Following injury induced by polysorbate lavage, rats in this group were maintained at a plateau pressure ( $P_{\text{high}} = 35\text{-}40$  cm  $\text{H}_2\text{O}$ ) for a time ( $T_{\text{high}} = 1.9\text{-}2.0$  seconds) that was set to occupy approximately 90% of the ventilatory cycle. The release pressure ( $P_{\text{low}} = 0$  cm  $\text{H}_2\text{O}$ ) was applied for a time ( $T_{\text{low}} = 0.13\text{-}0.40$  seconds). The  $T_{\text{low}}$  was adjusted so that the ratio of the end-expiratory flow rate (EEFR) to the peak expiratory flow rate (PEFR) was 10%, 25%, 50%, or 75%; larger values of the EEFR to PEFR ratio correspond to shorter  $T_{\text{low}}$ . This led to a mean (SEM) respiratory rate of 26.9 (0.2) breaths/min (EEFR to PEFR ratio of 10%) to 29.2 (0.3) breaths/min (EEFR to PEFR ratio of 75%). The rats were acclimated to each ventilator setting for 5 minutes prior to having in vivo microscopic fields recorded for 5 ventilator cycles.

### Analysis of Alveoli

Microscopic images of alveoli were recorded for analysis using StreamPix 5 (Norpix Inc). The dynamic changes in alveolar size during ventilation were determined by outlining individual alveoli at both peak inspiration and end expiration using PhotoShop CS6 (Adobe Inc). Individual alveolar areas were quantified using Image-Pro Plus (MediaCybernetics). The total alveolar air space area was calculated as a percentage of total frame area, with individual alveolar areas calculated in units of micrometers squared and individual alveolar radii calculated in units of micrometers. Alveoli that were visually lost between inspiration and expiration were assumed to have totally collapsed and were assigned areas of 0  $\mu\text{m}^2$  and radii of 0  $\mu\text{m}$ .

### Statistics

Results are reported as mean (standard error of the mean) values. Total alveolar air space occupancy was analyzed using analysis of variance, and the Dunnett multiple-comparison test was used for a post hoc comparison of each experimental group with the control group. We used the  $\chi^2$  test to compare the distribution of alveolar areas with the expected normal distribution to determine normality. The Kolmogorov-Smirnov test was performed to test for differences in distribution between the control group and the experimental groups, as well as between inspiration and expiration at each setting. All tests were 2-tailed, and  $P < .01$  was considered statistically significant. We used Prism version 5.0 statistical software for analysis (GraphPad Software Inc).

## Results

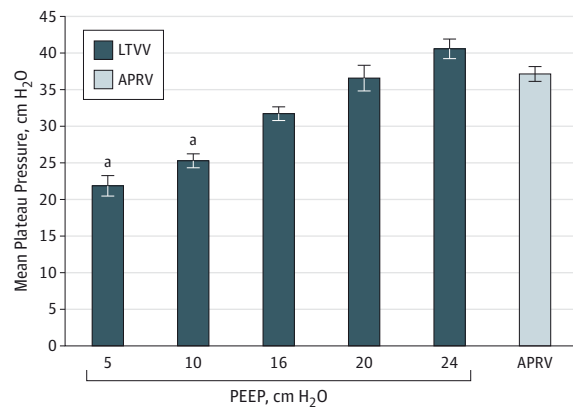
### Plateau Pressure

Increasing PEEP from 5 to 24 cm  $\text{H}_2\text{O}$  led to a concomitant increase in mean (SEM) plateau pressure from 21.9 (1.4) to 40.6 (1.3) cm  $\text{H}_2\text{O}$  (Figure 1). The mean (SEM) plateau pressures of the higher PEEPs of 16 to 24 cm  $\text{H}_2\text{O}$  (31.7 [0.9] to 40.6 [1.3] cm  $\text{H}_2\text{O}$ ) were statistically similar to those of APRV (37.1 [1.0] cm  $\text{H}_2\text{O}$ ;  $P > .01$ ).

### Alveolar Recruitment

There were significantly fewer alveoli at inspiration for low PEEP (5 and 10 cm  $\text{H}_2\text{O}$ ) in the 2 experimental groups com-

**Figure 1. Mean Plateau Pressures in Low Tidal-Volume Ventilation (LTVV) Group With Increasing Positive End-Expiratory Pressure (PEEP) and in Airway Pressure Release Ventilation (APRV) Group**



Error bars indicate standard error of the mean.

<sup>a</sup>  $P < .01$  vs APRV.

pared with the control group ( $P < .01$ ), whereas the number of alveoli per photomicrograph for all settings in the APRV group and a high PEEP (16-24 cm  $\text{H}_2\text{O}$ ) was not significantly different from the number of alveoli per photomicrograph in the control group ( $P > .01$ ; Table). At all settings of APRV, the number of alveoli at inspiration varied minimally with a range of mean (SEM) values of 46.0 (2.7) to 51.4 (5.4) alveoli per photomicrograph. By comparison, the mean (SEM) number of alveoli at inspiration in the LTVV group increased substantially with PEEP from 27.9 (6.5) (with a PEEP of 5 cm  $\text{H}_2\text{O}$ ) to 49.9 (4.1) (with a PEEP of 24 cm  $\text{H}_2\text{O}$ ) alveoli per photomicrograph. At expiration, there was a steady increase in the number of alveoli with increasing PEEP in the LTVV group, as well as with increasing EEFR to PEFR ratio in the APRV group, although it was not significantly different from the increase observed in the control group ( $P > .01$ ). The APRV group, with a longer expiratory duration (lower EEFR to PEFR ratio), demonstrated a reduction in the number of open alveoli at inspiration and expiration, whereas shorter expiratory durations (higher EEFR to PEFR ratio) increased the number of open alveoli at expiration and inspiration.

### Alveolar Diameter

The alveolar diameters at inspiration and expiration were similar between each of the experimental groups and the control group ( $P > .01$ ). Of the experimental settings tested, APRV with an EEFR to PEFR ratio of 75% trended toward the greatest alveolar radius at both inspiration and expiration. With an increasing PEEP and an increasing EEFR to PEFR ratio, the alveolar radius at expiration increased. With an EEFR to PEFR ratio of 50% or lower, there was a significant difference in alveolar radius between inspiration and expiration ( $P < .01$ ; Table).

### Alveolar Surface Area

The lower PEEP settings (5-16 cm  $\text{H}_2\text{O}$ ) in the 2 experimental groups had significantly less alveolar occupancy at both inspiration and expiration compared with those in the control

Table. Comparison of Alveolar Occupancy and Recruitment Between Control and Experimental Groups

Group	Mean (SEM)					
	Alveolar Occupancy, <sup>a</sup> %		No. of Alveoli		Alveolar Diameter, $\mu\text{m}$	
	Inspiration	Expiration	Inspiration	Expiration	Inspiration	Expiration
Control	53.3 (4.0)	50.3 (5.4)	60 (5.9)	55 (3.8)	39.0 (1.0)	36.4 (2.2)
APRV						
EEFR to PEFR ratio, %						
10	46.2 (2.8)	35.8 (2.4) <sup>b,c</sup>	51.4 (5.4)	32.8 (5.0)	38.4 (1.9)	26.2 (2.6) <sup>c</sup>
25	43.5 (2.3)	30.0 (2.7) <sup>b,c</sup>	46.0 (2.7)	31.9 (4.8)	40.2 (1.6)	27.0 (2.5) <sup>c</sup>
50	46.7 (2.8)	40.2 (3.2)	49.3 (3.2)	37.9 (4.8)	41.4 (1.2)	31.8 (1.8) <sup>c</sup>
75	47.9 (2.9)	46.6 (2.7)	50.6 (4.9)	45.4 (5.7)	40.1 (1.9)	38.8 (1.1)
LTVV						
PEEP, cm H <sub>2</sub> O						
5	24.8 (3.7) <sup>b</sup>	16.1 (4.1) <sup>b</sup>	27.9 (6.5) <sup>b</sup>	26.8 (7.7)	39.0 (5.1)	28.2 (5.2)
10	30.9 (3.1) <sup>b</sup>	24.0 (3.8) <sup>b</sup>	31.0 (4.6) <sup>b</sup>	33.6 (9.3)	39.1 (4.1)	30.7 (3.1)
16	32.7 (3.9) <sup>b</sup>	29.3 (3.6) <sup>b</sup>	33.5 (3.9)	35.4 (6.4)	34.1 (3.0)	31.2 (1.5)
20	39.9 (3.1)	35.9 (3.6)	40.1 (3.1)	38.1 (3.8)	37.3 (2.1)	34.4 (2.1)
24	42.2 (2.7)	38.7 (4.0)	49.9 (4.1)	45.1 (4.4)	38.9 (3.2)	32.7 (2.7)

Abbreviations: APRV, airway pressure release ventilation; EEFR, end-expiratory flow rate; LTVV, low tidal-volume ventilation; PEEP, positive end-expiratory pressure; PEFR, peak expiratory flow rate.

<sup>a</sup> Alveolar Occupancy represents the percentage of the photomicrograph occupied by alveolar area at inspiration and expiration. The experimental

groups include the LTVV group varying PEEP and the APRV group with increasing EEFR to PEFR ratios.

<sup>b</sup>  $P < .01$  (experimental group vs control group).

<sup>c</sup>  $P < .01$  (inspiration vs expiration).

group ( $P < .01$ ). Increasing PEEP to 20 and 24 cm H<sub>2</sub>O increased alveolar occupancy so that there was no significant difference in alveolar surface between the rats in the 2 experimental groups and the noninjured rats in the control group. At inspiration, the alveolar occupancy at all settings in the APRV group was statistically similar to the alveolar occupancy in the control group. At lower EEFR to PEFR ratios (10% and 25%), the alveolar occupancy at expiration in the 2 experimental groups was significantly less than that in the control group ( $P < .01$ ) and significantly less than the alveolar occupancy at inspiration ( $P < .01$ ; Table). Comparing all lung-injured rats at all ventilator settings, we found that APRV with an EEFR to PEFR ratio of 75% provided the greatest alveolar occupancy at both inspiration and expiration.

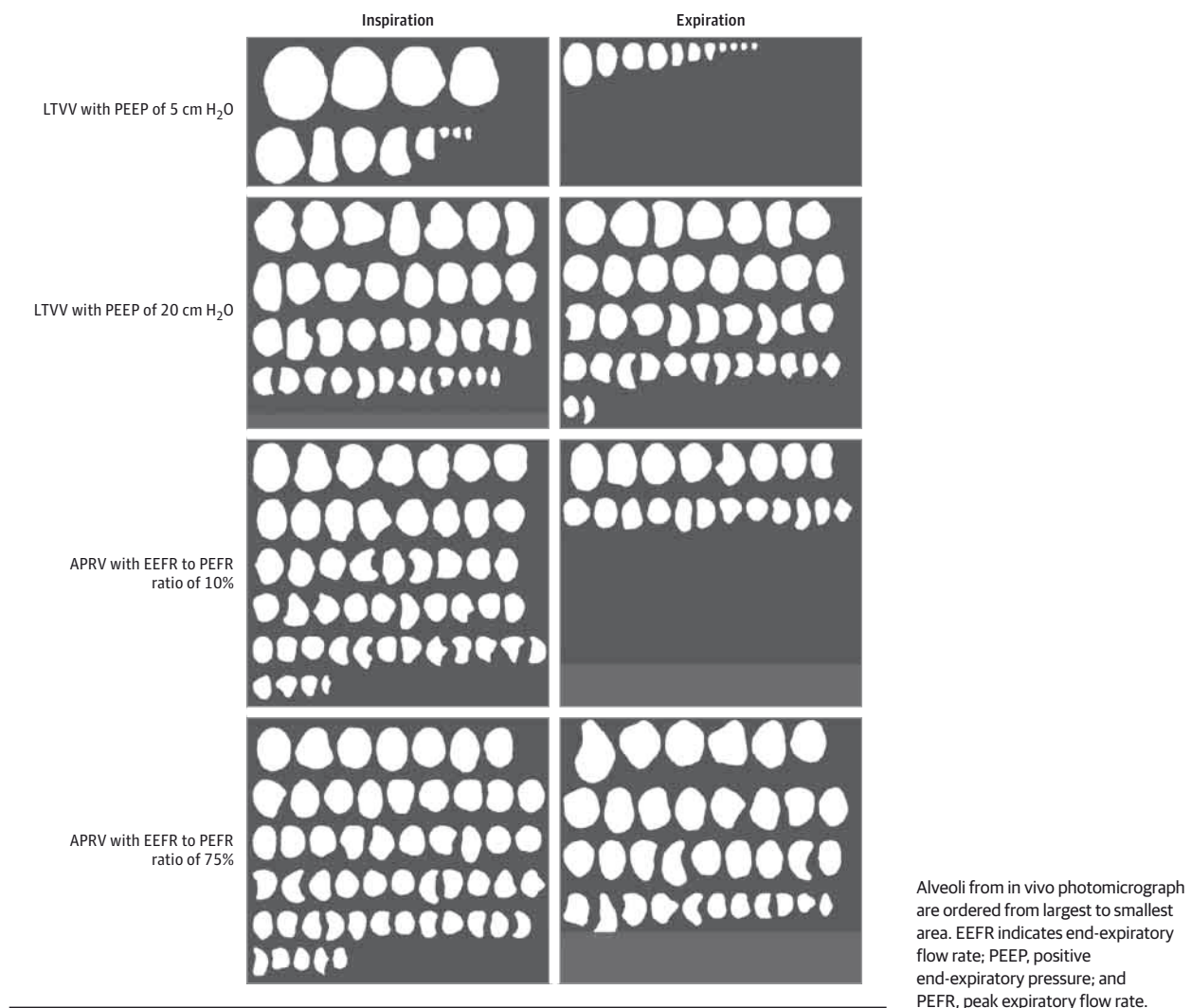
### Alveolar Heterogeneity

Qualitatively, there appeared to be greater dynamic heterogeneity with a PEEP of 5 cm H<sub>2</sub>O and an EEFR to PEFR ratio of 10%, whereas there was more dynamic homogeneity with a PEEP of 20 cm H<sub>2</sub>O and an EEFR to PEFR ratio of 75%, as shown for representative rats in Figure 2. At inspiration, the distribution of alveolar area also appeared to be similar between an EEFR to PEFR ratio of 10% and an EEFR to PEFR ratio of 75%. Using the  $\chi^2$  test, we compared the expected distribution of alveolar areas with the actual distribution. All groups failed the normality test. Using the Kolmogorov-Smirnov test, we compared the distributions of alveolar areas in the 2 experimental groups with the distribution of alveolar areas in the control group to determine whether the distributions were similar at both inspiration and expiration. At inspiration, all of the settings in the APRV group demonstrated an alveolar distribution similar to that observed in the control group ( $P > .01$ ;

Figure 3A), whereas none of the settings in the LTVV group demonstrated distributions that were similar to the distribution observed in the control group ( $P < .01$ ; Figure 3B). At expiration, neither of the experimental groups had an alveolar distribution similar to that of the control group ( $P < .01$ ; Figure 3C and D).

The Kolmogorov-Smirnov test was performed to determine dynamic heterogeneity, which reflects whether the alveolar size distributions significantly changed between inspiration and expiration in each group. In the control group, there was dynamic homogeneity ( $P > .01$ ), which indicates that there was not a significant change in the alveolar size distribution between inspiration and expiration as depicted in Figure 4A. In addition, there was minimal skew, with the median alveolar sizes at inspiration and expiration closely approximating the corresponding mean values. Likewise, the alveolar size distribution for all APRV settings at inspiration was characterized by low skew, with the median values closely approximating the alveolar mean values (Figure 4B-E). At expiration, there was positive skewness in the APRV group with EEFR to PEFR ratios of 10% (Figure 4B), which lessened with increasing EEFR to PEFR ratios. In the APRV group with low EEFR to PEFR ratios ( $\leq 50\%$ ), there was dynamic heterogeneity between inspiration and expiration ( $P < .01$ ), but there was dynamic homogeneity with an EEFR to PEFR ratio of 75% ( $P > .01$ ). In the LTVV group, the low PEEP settings (5 and 10 cm H<sub>2</sub>O; Figure 4F-G) also demonstrated positive skewness at expiration, which lessened with increasing PEEP (16-24 cm H<sub>2</sub>O; Figure 4H-J). The low PEEP settings (5 and 10 cm H<sub>2</sub>O) demonstrated dynamic heterogeneity between inspiration and expiration ( $P < .01$ ), but with increasing PEEP (16-24 cm H<sub>2</sub>O), there was a closer approximation of both the alveolar mean and median values be-

**Figure 2. Qualitative Comparison of Dynamic Alveolar Heterogeneity Between Inspiration and Expiration at Low Tidal-Volume Ventilation (LTVV) and at Airway Pressure Release Ventilation (APRV)**



tween inspiration and expiration, which indicates dynamic homogeneity ( $P > .01$ ).

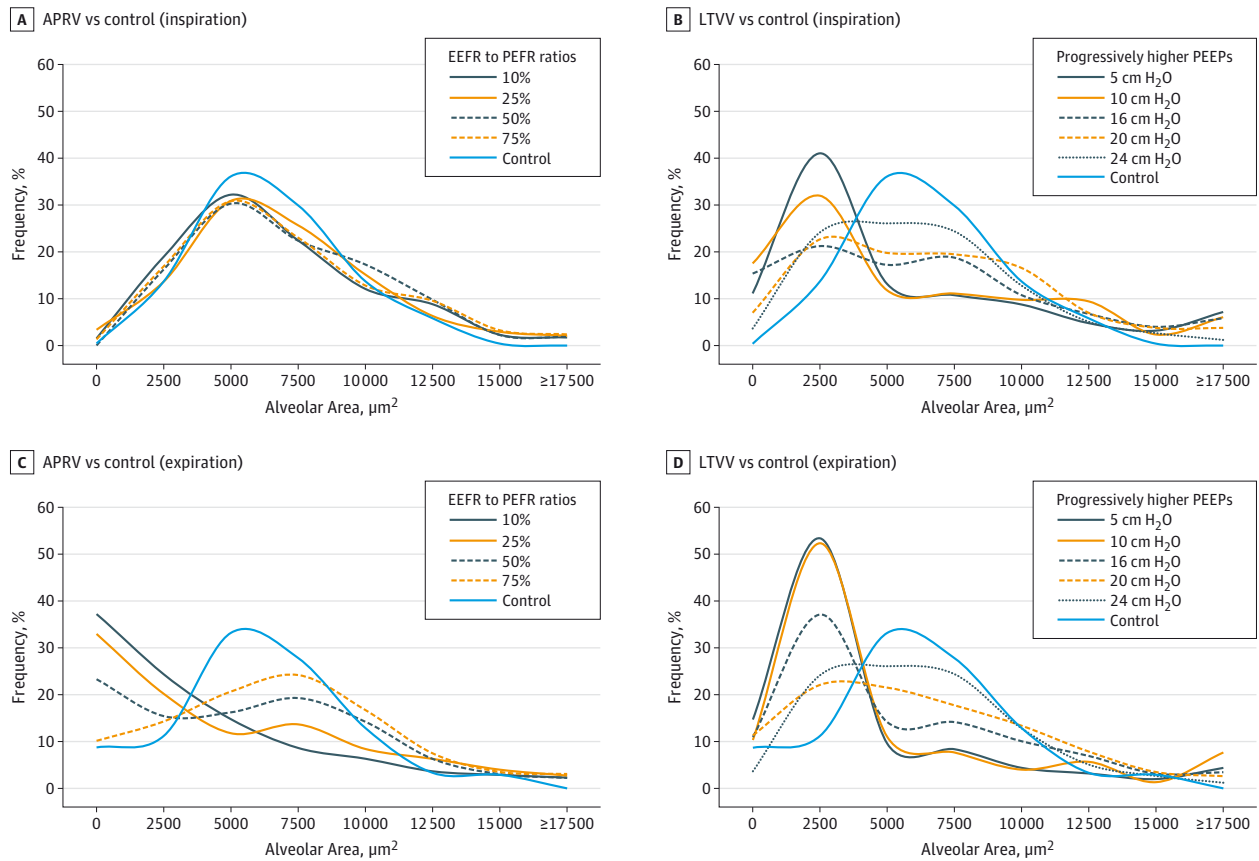
## Discussion

In most investigations into the pathogenesis of ventilator-induced lung injury, the assessment of heterogeneity is made at the level of the whole lung.<sup>6,7</sup> This represents a length scale several orders of magnitude larger than that of the alveoli, which are directly affected by the stresses and strains of mechanical ventilation<sup>16</sup> and, therefore, might not accurately reflect the alveolar heterogeneity that occurs in the injured lung.<sup>17</sup> Applying a mechanical breath to a heterogeneous population of alveoli might result in localized regions of high stress without a significant increase in the overall stress of the whole lung.<sup>6</sup> Likewise, the changes in alveolar size distribution at inspiration vs expiration that occur when dynamic heterogeneity is present are indicative of abnormal alveolar microstrain<sup>5</sup> and

intratidal derecruitment, which are known to accelerate the progression of lung injury. Thus, to truly identify the protective benefits of a ventilation strategy, the spatiotemporal alveolar heterogeneity that it causes must be assessed. Using computational modeling,<sup>10</sup> we have recently shown evidence that both alveolar microstrain and intratidal derecruitment depend markedly on ventilator settings for both LTVV and APRV. The results of the present study directly corroborate these previous modeling results and confirm the importance of ventilating the injured lung in a manner that minimizes the heterogeneous mechanical behavior of the lung at the level of individual alveoli.

The normal lung is homogeneously expanded near total lung capacity.<sup>18</sup> Accordingly, the inspiratory pressure used in APRV is conventionally set to produce lung volumes at a point on the steep portion of the pressure-volume curve that is well above functional residual capacity but still less than total lung capacity. This avoids alveolar overdistension and encourages spontaneous breathing by patients while, at the same time, promot-

Figure 3. Comparison of Alveolar Distributions at Inspiration vs Expiration in Experimental Groups vs Control Group



A, All of the settings (ie, ratios of end-expiratory flow rate [EEFR] to peak expiratory flow rate [PEFR]) in the airway pressure release ventilation (APRV) group demonstrated an alveolar distribution similar to that observed in the control group at inspiration ( $P > .01$ ). B, None of the settings (ie, progressively higher positive end-expiratory pressures [PEEPs]) in the low tidal-volume

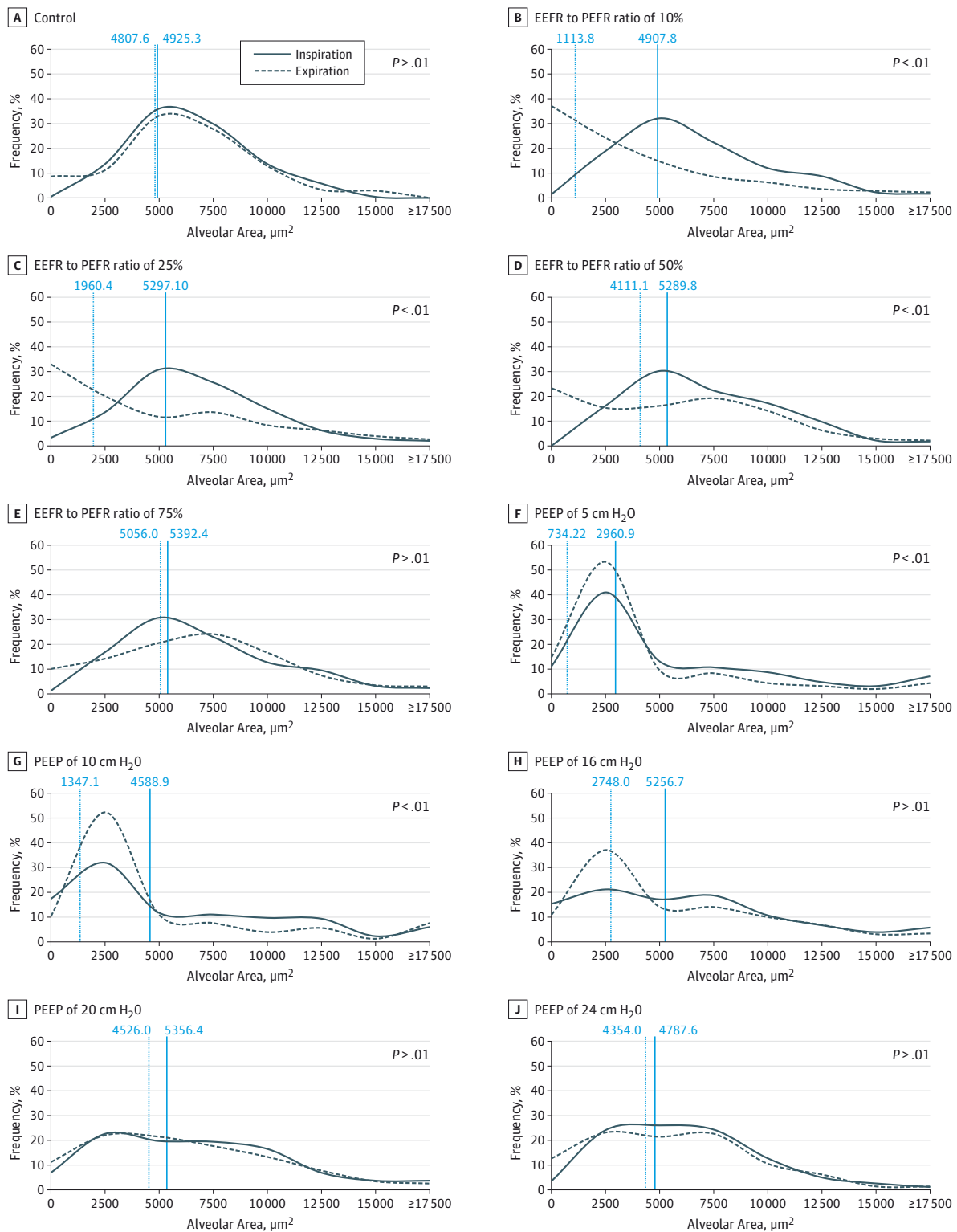
ventilation (LTVV) group at inspiration demonstrated distributions that were similar to the distribution observed in the control group ( $P < .01$ ). C and D, None of the settings at expiration (ie, progressively higher PEEPs or EEFR to PEFR ratios) in either experimental group demonstrated distributions that were similar to the distributions observed in the control group ( $P < .01$ ).

ing alveolar recruitment.<sup>19</sup> The ability of APRV to maintain alveolar homogeneity thus arises because the majority (approximately 90%) of the ventilation cycle is spent at the upper pressure ( $P_{high}$ ).<sup>18</sup> The sustained greater lung volume that this produces results in alveolar size distributions for APRV at inspiration that are independent of the value of  $T_{low}$ , as shown in Figures 2 and 3. These size distributions are also similar to those observed in control animals randomly assigned to LTVV, which shows that APRV did not cause additional alveolar overdistension. In contrast, the alveolar size distribution for APRV at expiration is highly dependent on  $T_{low}$ . In particular, an EEFR to PEFR ratio of 50% or lower caused a marked decrease in the median alveolar size, increased derecruitment, and resulted in a positive skew of the size distribution similar to that of decreasing PEEP with LTVV (Figure 4). In other words, longer durations at  $P_{low} = 0$  cm H<sub>2</sub>O allowed sufficient time for significant derecruitment to occur with each expiration. The benefits of APRV in terms of increased homogeneity and decreased intratidal derecruitment that have been reported in human studies<sup>20</sup> and in animal models of ARDS<sup>5,21-23</sup> thus require that  $T_{low}$  be set appropriately such that the EEFR to PEFR ratio is 75%.

These findings are supported by an experimental study<sup>24</sup> demonstrating that a prolonged inspiratory time at the plateau pressure requires either an expiratory phase of a brief duration to a low pressure or an expiratory phase of a longer duration to a high pressure in order to stabilize oleic-acid-injured lungs.

Manipulating the parameters of conventional LTVV in the injured rats also had a substantial effect on dynamic alveolar heterogeneity. For example, a low PEEP decreased the median alveolar size in a manner similar to prolonged  $T_{low}$  in APRV (Figure 4). The positive skew in the alveolar distributions at low PEEPs indicates that the rats that underwent ventilator-induced lung injury by polysorbate-induced surfactant deactivation required increased airway pressures in order to maintain the presumably normal alveolar architecture exhibited by the uninjured rats in the control group. Furthermore, the significantly lower number of patent alveoli (Table) observed in the rats ventilated with low PEEP indicate that the resulting low ventilation pressures were not sufficient to maintain recruitment following lung injury. Increasing PEEP, which resulted in increased inspiratory pressures due to the fixed  $V_t$ , reduced the skewness of the alveolar distributions at inspira-

Figure 4. Alveolar Distributions at Inspiration and Expiration



Comparison of alveolar distributions between inspiration and expiration in the control group (A), the airway pressure release ventilation group with increasing ratio of end-expiratory flow rate (EEFR) to peak expiratory flow rate (PEFR) (B-E), and the low tidal-volume ventilation group with increasing positive end-expiratory pressure (PEEP) (F-J). Alveolar distribution at inspiration (solid curve) is compared with alveolar distribution at expiration (dotted curve).

Median values are represented by the 2 vertical lines (solid line = median at inspiration; dotted line = median at expiration).  $P < .01$  indicates statistical significance for dynamic heterogeneity (dissimilar alveolar distributions between inspiration and expiration), and  $P > .01$  indicates dynamic homogeneity.

tion and promoted dynamic alveolar homogeneity (Figure 4). Therefore, the improvements in homogeneity with PEEP might have been due to a combination of increased plateau and end-expiratory pressures (Figure 1) that would have induced alveolar recruitment and prevented derecruitment.

Another interesting possible effect of PEEP, suggested by Namati et al,<sup>25</sup> is that it **might facilitate recruitment via the pores of Kohn**. Opening the pores of Kohn, therefore, might enable **collateral ventilation** and allow for the redistribution of alveolar volume from more compliant to adjacent, less-compliant alveoli, thereby promoting alveolar homogeneity.<sup>25</sup> Corroborating this hypothesis, Wellman et al,<sup>26</sup> using positron emission tomography, established that increasing PEEP in a sheep nitrogen washout model improved specific ventilation homogeneity. In the present study, increasing the end-expiratory lung volume by either increasing PEEP or increasing the EEFR to PEFR ratio increased alveolar occupancy at expiration and decreased alveolar derecruitment (Table). Increasing PEEP also led to an increase in alveolar occupancy, although not to the same degree as APRV at inspiration, likely because the prolonged  $T_{\text{high}}$  in APRV allowed time for nearly complete recruitment of alveoli.

The distributions of alveolar areas observed in the control and experimental groups were non-Gaussian. Mazzuca et al<sup>17</sup> hypothesized that such non-Gaussian distributions are artifacts because in vivo microscopy does not evaluate each alveolus in the plane of the alveolar centroid. Alternatively, Namati et al<sup>25</sup> suggested that non-Gaussian distributions observed using a laser-scanning confocal technique were the result of evaluating 3 types of alveoli: those that change with tidal inflation, those that do not, and those that collapse at expiration. These effects are exaggerated in lung injuries associated with the loss of surfactant function<sup>27</sup> due to elevated rates and magnitudes of derecruitment.<sup>9</sup> In any case, the alveolar size distributions in the present study were significantly positively skewed at low pressures (Figure 4), similar to the skewed size distributions observed using in vivo microscopy in open-chest rabbits at 3 cm H<sub>2</sub>O.<sup>17</sup> Likewise, our distributions at high PEEP (20 and 24 cm H<sub>2</sub>O; Figure 4) demonstrate the same decrease in kurtosis (or flattening of the curve) as observed by Mazzuca et al<sup>17</sup> at a pressure of 16.5 cm H<sub>2</sub>O.

The experimental findings of the present study thus provide direct evidence that alveolar heterogeneity is reduced by increases in lung inflation pressure. Nevertheless, these findings must still be viewed in the context of the limitations of the in vivo microscopy technique and the region of the lung studied. Ventilation heterogeneity exists across the lung, and our assessment was limited to zone I, or the anterior surface, of the lung and therefore may not necessarily be generalized to the whole lung. One other potential issue is that suction is re-

quired to stabilize the lung tissue on the microscope coverslip during imaging, and this is known to increase both alveolar stability and size. These effects appear, however, to be subtle.<sup>28</sup> Another potentially significant limitation is that in vivo microscopy can only evaluate subpleural alveoli to a depth of approximately 70  $\mu\text{m}$ . This restricts investigation essentially to 2 dimensions and does not allow for the characterization of the gas distribution to the conducting air spaces. However, the normalization of the alveolar size distribution with increasing airway pressure, as we found in the present study (Figure 4), has also been found using a laser-scanning confocal technique capable of looking deeper into excised mouse lungs.<sup>25</sup> Furthermore, similar improvements in lung homogeneity with increasing PEEP and plateau pressure have been observed using computed tomography in patients with ARDS,<sup>6</sup> so it seems reasonable to propose that the behavior of subpleural alveoli, as observed by in vivo microscopy, provides a suitable approximation of whole-lung alveolar dynamics. Finally, it must be remembered that the mechanics of lungs in a patient with ARDS is influenced by the presence of an intact chest wall, diaphragm, and abdomen.<sup>18,29</sup> In the present study, the chest wall was removed, as necessitated by the use of in vivo microscopy, so conditions were not identical to those encountered clinically.

## Conclusions

The alveolar size distributions observed using in vivo microscopy in lung-injured rats demonstrate the importance of both the magnitude and the duration of the applied pressures during mechanical ventilation. The extended durations of APRV at the inspiratory pressure ( $T_{\text{high}}$ ) provide alveolar size distributions at inspiration that closely approximate noninjured rats ventilated at low tidal volumes ( $P > .01$ ). For long durations of  $T_{\text{low}}$  (EEFR to PEFR ratio of  $\leq 50\%$ ), significant changes in the alveolar size distribution occur from inspiration to expiration, which reflect dynamic alveolar heterogeneity. Reducing the APRV  $T_{\text{low}}$  duration (EEFR to PEFR ratio of 75%) eliminates this dynamic heterogeneity and reduces intratidal derecruitment, providing a close approximation of the dynamics observed in the control group. Likewise, increasing PEEP during LTVV increases recruitment, alveolar occupancy, and dynamic homogeneity. However, even at a PEEP of 24 cm H<sub>2</sub>O, the alveolar size distributions at inspiration are significantly different from the alveolar size distribution observed in the control group. Our findings indicate that the alveolar dynamics during APRV with an EEFR to PEFR ratio of 75% more closely resembles the dynamics of a healthy lung than does the alveolar dynamics during LTVV with a PEEP of up to 24 cm H<sub>2</sub>O.

### ARTICLE INFORMATION

**Accepted for Publication:** June 7, 2015.

**Published Online:** October 7, 2015.  
doi:10.1001/jamasurg.2015.2683.

**Author Contributions:** Dr Kollisch-Singule and Mr Satalin had full access to all of the data in the study

and take responsibility for the integrity of the data and the accuracy of the data analysis.

**Study concept and design:** Kollisch-Singule, Andrews, Roy, Meng, Gatto, Nieman, Habashi.  
**Acquisition, analysis, or interpretation of data:** Kollisch-Singule, Jain, Andrews, Smith, Hamlington-Smith, Roy, DiStefano, Nuss, Satalin, Meng, Marx, Bates, Gatto, Habashi.

**Drafting of the manuscript:** Kollisch-Singule, Andrews, DiStefano, Nuss, Meng, Marx, Gatto, Nieman, Habashi.

**Critical revision of the manuscript for important intellectual content:** Jain, Andrews, Smith, Hamlington-Smith, Roy, Satalin, Marx, Bates, Gatto, Nieman, Habashi.

*Statistical analysis:* Jain, DiStefano, Nuss, Meng, Gatto.

*Obtained funding:* Nieman.

*Administrative, technical, or material support:* Kollisch-Singule, Jain, Roy, Nuss, Satalin, Meng, Gatto.

*Study supervision:* Roy, Satalin.

**Conflict of Interest Disclosures:** None reported.

**Funding/Support:** This work was supported by a seed grant from the American Medical Association Foundation.

**Role of the Funder/Sponsor:** The American Medical Association Foundation had no role in the design and conduct of the study; collection, management, analysis, or interpretation of the data; preparation, review, or approval of the manuscript; and decision to submit the manuscript for publication.

**Previous Presentation:** This paper was presented at the 39th Annual Meeting of the Association of VA Surgeons; May 4, 2015; Miami Beach, Florida.

## REFERENCES

- Ware LB, Matthay MA. The acute respiratory distress syndrome. *N Engl J Med*. 2000;342(18):1334-1349.
- Herridge MS, Tansey CM, Matté A, et al; Canadian Critical Care Trials Group. Functional disability 5 years after acute respiratory distress syndrome. *N Engl J Med*. 2011;364(14):1293-1304.
- Tsuchida S, Engelberts D, Peltekova V, et al. Atelectasis causes alveolar injury in nonatelectatic lung regions. *Am J Respir Crit Care Med*. 2006;174(3):279-289.
- Mead J, Takishima T, Leith D. Stress distribution in lungs: a model of pulmonary elasticity. *J Appl Physiol*. 1970;28(5):596-608.
- Kollisch-Singule M, Emr B, Smith B, et al. Mechanical breath profile of airway pressure release ventilation: the effect on alveolar recruitment and microstrain in acute lung injury. *JAMA Surg*. 2014; 149(11):1138-1145.
- Cressoni M, Cadringer P, Chiurazzi C, et al. Lung inhomogeneity in patients with acute respiratory distress syndrome. *Am J Respir Crit Care Med*. 2014; 189(2):149-158.
- Zhao Z, Pullet S, Frerichs I, Müller-Lisse U, Möller K. The EIT-based global inhomogeneity index is highly correlated with regional lung opening in patients with acute respiratory distress syndrome. *BMC Res Notes*. 2014;7:82.
- Massa CB, Allen GB, Bates JH. Modeling the dynamics of recruitment and derecruitment in mice with acute lung injury. *J Appl Physiol*. 2008;105(6):1813-1821.
- Smith BJ, Grant KA, Bates JH. Linking the development of ventilator-induced injury to mechanical function in the lung. *Ann Biomed Eng*. 2013;41(3):527-536.
- Smith BJ, Lundblad LK, Kollisch-Singule M, et al. Predicting the response of the injured lung to the mechanical breath profile. *J Appl Physiol*. 2015;118(7):932-940.
- Pavone L, Albert S, DiRocco J, Gatto L, Nieman G. Alveolar instability caused by mechanical ventilation initially damages the nondependent normal lung. *Crit Care*. 2007;11(5):R104.
- Schmidt R, Meier U, Yabut-Perez M, et al. Alteration of fatty acid profiles in different pulmonary surfactant phospholipids in acute respiratory distress syndrome and severe pneumonia. *Am J Respir Crit Care Med*. 2001;163(1):95-100.
- Davidson BA, Knight PR, Wang Z, et al. Surfactant alterations in acute inflammatory lung injury from aspiration of acid and gastric particulates. *Am J Physiol Lung Cell Mol Physiol*. 2005;288(4):L699-L708.
- Nieman GF, Clark WR Jr, Wax SD, Webb SR. The effect of smoke inhalation on pulmonary surfactant. *Ann Surg*. 1980;191(2):171-181.
- Pelosi P, D'Onofrio D, Chiumello D, et al. Pulmonary and extrapulmonary acute respiratory distress syndrome are different. *Eur Respir J Suppl*. 2003;42:48s-56s.
- Hubmayr RD. Perspective on lung injury and recruitment: a skeptical look at the opening and collapse story. *Am J Respir Crit Care Med*. 2002;165(12):1647-1653.
- Mazzuca E, Salito C, Rivolta I, Aliverti A, Miserocchi G. From morphological heterogeneity at alveolar level to the overall mechanical lung behavior: an in vivo microscopic imaging study. *Physiol Rep*. 2014;2(2):e00221.
- Chevalier PA, Rodarte JR, Harris LD. Regional lung expansion at total lung capacity in intact vs. excised canine lungs. *J Appl Physiol Respir Environ Exerc Physiol*. 1978;45(3):363-369.
- Habashi NM. Other approaches to open-lung ventilation: airway pressure release ventilation. *Crit Care Med*. 2005;33(3 suppl):S228-S240.
- Andrews PL, Shiber JR, Jaruga-Killeen E, et al. Early application of airway pressure release ventilation may reduce mortality in high-risk trauma patients: a systematic review of observational trauma ARDS literature. *J Trauma Acute Care Surg*. 2013;75(4):635-641.
- Roy SK, Emr B, Sadowitz B, et al. Preemptive application of airway pressure release ventilation prevents development of acute respiratory distress syndrome in a rat traumatic hemorrhagic shock model. *Shock*. 2013;40(3):210-216.
- Roy S, Sadowitz B, Andrews P, et al. Early stabilizing alveolar ventilation prevents acute respiratory distress syndrome: a novel timing-based ventilatory intervention to avert lung injury. *J Trauma Acute Care Surg*. 2012;73(2):391-400.
- Kollisch-Singule M, Emr B, Smith B, et al. Airway pressure release ventilation reduces conducting airway micro-strain in lung injury. *J Am Coll Surg*. 2014;219(5):968-976.
- Neumann P, Berglund JE, Mondéjar EF, Magnusson A, Hedenstierna G. Effect of different pressure levels on the dynamics of lung collapse and recruitment in oleic-acid-induced lung injury. *Am J Respir Crit Care Med*. 1998;158(5, pt 1):1636-1643.
- Namati E, Thiesse J, de Ryk J, McLennan G. Alveolar dynamics during respiration: are the pores of Kohn a pathway to recruitment? *Am J Respir Cell Mol Biol*. 2008;38(5):572-578.
- Wellman TJ, Winkler T, Costa EL, et al. Measurement of regional specific lung volume change using respiratory-gated PET of inhaled <sup>13</sup>N-nitrogen. *J Nucl Med*. 2010;51(4):646-653.
- Bates JHT, Irvin CG. Time dependence of recruitment and derecruitment in the lung: a theoretical model. *J Appl Physiol (1985)*. 2002;93(2):705-713.
- Pavone LA, Albert S, Carney D, Gatto LA, Halter JM, Nieman GF. Injurious mechanical ventilation in the normal lung causes a progressive pathologic change in dynamic alveolar mechanics. *Crit Care*. 2007;11(3):R64.
- Hubmayr RD, Rodarte JR, Walters BJ, Tonelli FM. Regional ventilation during spontaneous breathing and mechanical ventilation in dogs. *J Appl Physiol (1985)*. 1987;63(6):2467-2475.